Revista Mexicana de Astronomía y Astrofísica, **33**, 187–195 (1997)

KARHUNEN-LOEVE FUNCTIONS IN SIMULATIONS OF ATMOSPHERIC DISTORTIONS

V. G. Orlov, V. V. Voitsekhovich, and S. Cuevas

Instituto de Astronomía
Universidad Nacional Autónoma de México

Received 1997 May 31; accepted 1997 September 9

RESUMEN

Se considera el problema de la simulación de frentes de onda con distorsiones producidas por la turbulencia atmosférica, utilizando las funciones de Karhunen-Loeve, para el estudio de técnicas de alta resolución espacial en astronomía. Se encuentra una solución analítica para el kernel de la ecuación integral de Karhunen-Loeve para el caso de la turbulencia de Kolmogorov con una escala externa finita. Se consideraran dos modelos de escala externa: el modelo exponencial y el modelo de von Karman. Se describe un generador que permite simular procesos aleatorios isotrópicos en dos dimensiones. Se muestra que los dos modelos dan resultados similares.

ABSTRACT

The problem of simulations of the atmospherically distorted wavefronts, making use of Karhunen-Loeve functions for the study of high resolution techniques in astronomy is considered. An analytic solution for the kernel of the Karhunen-Loeve integral equation is found for the case of Kolmogorov turbulence with a finite outer-scale length. Two outer-scale models are considered: the exponential model and the von Karman model. A generator allowing the simulation of two-dimensional isotropic random processes with a given structure function is described. It is shown that both considered models give nearly the same results.

Key words: **ATMOSPHERIC EFFECTS — METHODS–NUMERICAL — TELESCOPES — TURBULENCE**

1. INTRODUCTION

The optical quality of earth based telescopes is never diffraction limited; this is due to two main reasons: the atmospheric turbulence wavefront distortions and the intrinsic quality of the telescope optics which is, in most of the cases, comparable to the atmospheric distortions (Roddier et al. 1994). Active optics has resolved this last problem and, at the same time, reduced the cost of large telescopes (Wilson, Franza, & Noethe 1987). In order to obtain diffraction limited imaging of different stellar objects, despite the turbulence induced atmospheric distortions, the speckle interferometry (Labeyrie 1970) and adaptive optics techniques (Babcock 1953) have been proposed. There are many examples of important astronomical results obtained at visible wavelengths in speckle interferometry by different speckle techniques (Pehlemann, Hofmann, & Weigelt 1992; Afanasiyev et al. 1992) and at the infrared by the use of adaptive optics (Rigaut & Gehring 1995; Roddier et al. 1996; Close et al. 1997). There are many publications devoted to the theoretical analysis of these methods (Roddier 1981; Alloin & Mariotti 1988; 1993). However, there are many problems where it is difficult to apply a pure analytical treatment. For this reason, different types of simulators that allow the generation of random wavefront distortions with given statistics, have been developed. These simulators are of help when, for example, it is necessary to estimate performances of closed-loop adaptive correction where a complete theoretical treatment becomes extremely complicated. Another advantage of simulations is the possibility to analyze particular samples of the process of interest while a theory is always dealing with statistical quantities.

It is usually assumed that the atmospheric wavefront distortions obey Kolmogorov statistics. This assumption allows to simplify significantly a theoretical treatment and a simulation procedure as well. Firstly, an idea of quasi-random simulations of the wavefront distortions has been proposed by McGlameri (1976) as follows: at first, random phases are produced over the pupil, then the atmospheric statistics is introduced with proper filtering by the Kolmogorov spectrum. However, this procedure has two drawbacks: low-order aberrations are underestimated and a long time is required for simulations that make it less desirable for many applications.

Another approach has been developed by Roddier (1990), who used the Zernike polynomial expansion of wavefront distortions to produce random wavefront samplings with Kolmogorov statistics. In this case, a correlation matrix of Zernike coefficients is known from theory (Noll 1976), so application of a proper numerical diagonalization procedure yields a new set of basis functions for which the expansion coefficients are statistically-independent. Actually, this procedure gives us a set of the so-called Karhunen-Loeve (K-L) functions that are well-known in probability theory (Loeve 1955; Papoulis 1984). Such set of functions is convenient for simulations because each coefficient can be generated independently. Firstly the K-L functions for Kolmogorov wavefront statistics have been calculated by Wang & Markey (1978). In order to construct this set, one needs to solve the homogeneous integral equation with a kernel given by the correlation function of a random process to be simulated. An usage of these functions in computer simulations has been considered by Cannon (1996), who developed a wavefront simulator applying a direct numerical solution of the K-L equation.

All the simulators above operate on the base of Kolmogorov turbulence model which involves a conception of infinite outer scale of the turbulence. However, recent experimental data (Bouricius & Clifford 1970; Clifford et al. 1971; Coulman et al. 1988; Nightingale & Buscher 1991; Bester et al. 1992; Dekens et al. 1994; Buscher et al. 1995) leads us to conclude that the outer scale has often a finite size ranging from some meters to some tens of meters. Theoretical considerations show that under such conditions, the atmosphere affects astronomical images in a different way than it would in the case of Kolmogorov turbulence (Voitsekhovich 1995; Voistekhovich & Cuevas 1995; Takato & Yamaguchi 1995; Winker 1991). The effect of finite outer scale is very significant in large telescopes and interferometric telescope arrays. Thus, one needs to consider the outer scale-dependent turbulence models for adequate simulation of atmospherically-induced wavefront distortions.

The present paper describes a simulator which allows the generation of wavefront distortions for both the case of finite and infinite outer scale. Such simulations are needed for modelling of the performance of modern astronomical instruments: image quality to be obtained by large-size ground-based telescopes, adaptive optics systems for big telescopes, long-based interferometry, speckle interferometry with partial adaptive correction, etc. Two outer-scale-dependent models are considered: the von Karman model and the exponential model. The K-L functions for both models are constructed on the basis of Zernike polynomial expansion. This approach permits a reduction of the integral K-L equation to a system of linear algebraic equations for which the matrix elements are expressed analytically in terms of hypergeometric functions. These analytical expressions are of importance because they give the possibility of combining a desired accuracy with high speed of simulations. The practicability of the simulator developed is illustrated by comparison of the simulation results and the theoretical ones.

2. KARHUNEN-LOEVE FUNCTIONS AS A BASIS FOR MODELLING RANDOM PROCESSES

Let us assume that one needs to simulate two-dimensional turbulence-induced phase distortions $S\left(\vec{\rho}\right)$ at the circular telescope pupil with radius R. Then, let $S\left(\vec{\rho}\right)$ be expanded over a set of some basic functions $\Lambda_i(\vec{\rho})$ orthogonal over the unit circle

$$S(\vec{\rho}) = \sum_i \alpha_i \Lambda_i\left(\vec{\rho}/R\right) \quad , \tag{1}$$

$$\int_{G_R} \mathrm{d}^2\rho\, \Lambda_i\left(\vec{\rho}/R\right) \Lambda_j\left(\vec{\rho}/R\right) = \pi R^2 \delta_{ij} \quad , \tag{2}$$

where δ_{ij} is the Kronecker delta-symbol. Hereafter the subscript G_R denotes the integration over the aperture.

Taking into account the orthogonal properties (2), the coefficients α_i can be expressed as

$$\alpha_i = \frac{1}{\pi R^2} \int_{G_R} \mathrm{d}^2\rho S\left(\vec{\rho}\right) \Lambda_i\left(\vec{\rho}/R\right) \tag{3}$$

Furthermore, let us choose the functions Λ_i in such a way that the following condition holds

$$\langle a_i a_j \rangle = \lambda_{ij}^2 \delta_{ij} \quad , \tag{4}$$

where λ_{ij} is the normalization factor.

The functions Λ_i satisfying eqs. (2–4) are called the Karhunen-Loeve (K-L) functions (Papoulis 1984) of the random process S. According to the K-L theorem, the functions Λ_i are found from the following homogeneous integral equation (in what follows, K-L equation)

$$\int_{G_R} \mathrm{d}^2\rho B_S\left(\vec{\rho_1}, \vec{\rho_2}\right) \Lambda\left(\vec{\rho_1}/R\right) = \lambda^2 \Lambda\left(\vec{\rho_2}/R\right) \quad , \tag{5}$$

where B_S is the correlation function of phase S.

The correlation function B_S associated with turbulence-induced phase distortions is always symmetric. Hence, as it is known from the theory of integral equations, the eigenfunctions Λ_i and eigenvalues λ_i hold the following general properties: *(i)* The system of the eigenfunctions is complete; *(ii)* The eigenfunctions are real and orthogonal; *(iii)* The eigenvalues are positive.

These properties along with statistical orthogonality given by eq. (4) make the K-L functions to be very convenient for modelling random process. Once the K-L functions associated with a given random process are calculated, it is easy to generate samplings of this process taking the superposition of K-L functions with random coefficients (the standard variances of the coefficients must be equal to the corresponding eigenvalues λ_i)

In the general case, if one needs to calculate the two-dimensional K-L functions, a solution of the eq. (5) turns out to be quite non-trivial. Nevertheless, the turbulence-induced wavefront distortions are assumed to be isotropic (Tatarski 1961), and that allows reduction of the initial two-dimensional problem to the one-dimensional case. Due to the isotropy the correlation function B_S in eq. (5) depends only on the separation between the points $\vec{\rho_1}$ and $\vec{\rho_2}$, i.e., $B_S(\vec{\rho_1}, \vec{\rho_2}) = B_S(|\vec{\rho_1} - \vec{\rho_2}|)$. Hence, the functions Λ_i in polar coordinates can be presented as a product of the angular and radial parts

$$\Lambda_i(\vec{\rho}/R) = L_n^m(\rho/R)\Theta^m(\varphi) \quad , \tag{6}$$

where

$$\Theta^m(\varphi) = \begin{cases} \cos(m\varphi) & i \text{ is even}, \quad m \neq 0, \\ \sin(m\varphi) & i \text{ is odd}, \quad m \neq 0, \\ 1 & m = 0. \end{cases} \tag{7}$$

The correlation function B_S can be written as (Voistekhovich & Cuevas 1995)

$$B_S(\rho_1, \rho_2) = 0.49 r_0^{-5/3} \int \mathrm{d}^2\varkappa \Phi_n(\varkappa) \exp\left[i\,\vec{\varkappa}\left(\vec{\rho_1} - \vec{\rho_2}\right)\right], \tag{8}$$

where Φ_n denotes the spectrum of refractive-index fluctuations, and r_0 denotes the Fried parameter (Fried 1966).

Substituting expressions (6–8) into (5) and calculating the integrals, we obtain the following one-dimensional integral equation for the radial K-L functions $L_n^m\,(\rho/R)$

$$\int_0^R L_n^m\left(\rho_1/R\right) K\left(\rho_1, \rho_2\right) \rho_1\, d\rho_1 = \lambda_{n,m}^2 L_n^m\left(\rho_2/R\right) \quad , \tag{9}$$

with the kernel $K\left(\rho_1, \rho_2\right)$ given by

$$K\left(\rho_1, \rho_2\right) = 1.96\pi r_0^{-5/3} R^{-2} \int_0^\infty \mathrm{d}\varkappa \varkappa \Phi_n(\varkappa) J_m\left(\varkappa\rho_1\right) J_m\left(\varkappa\rho_2\right), \tag{10}$$

where J_m denotes the Bessel function.

Then, let us find the functions L_n^m as a linear superposition of the radial Zernike polynomials R_j^m

$$L_n^m(\rho) = \sum_{j=m}^{\infty} \beta_{j,n}^m \sqrt{2j+2} R_j^m(\rho) \quad , \tag{11}$$

where

$$R_n^m(\rho) = \sum_{s=0}^{(n-m)/2} \frac{(-1)^s (n-s)!}{s!\left[(n+m)/2 - s\right]!\left[(n-m)/2 - s\right]!} \rho^{n-2s} \tag{12}$$

Substituting eq. (11) into eq. (9), multiplying the equation obtained by $\rho_2 R_k^m(\rho_2/R)$ and performing the integration over ρ_1 and ρ_2, we get the following homogeneous system of algebraic equations for the coefficients $\beta_{j,n}^m$

$$\sum_j \beta_{j,n}^m A_{j,i}^m = \lambda_m^2 \beta_{i,n}^m \quad , \tag{13}$$

where

$$\begin{aligned} A_{j,i}^m &= 3.92\pi R^{-2} r_0^{-5/3} (-1)^{(i+j-2m)/2} (1-\delta_{0i})(1-\delta_{0j})\sqrt{(i+1)(j+1)} \\ &\times \int_0^\infty d\varkappa \varkappa^{-1} \Phi_n(\varkappa) J_{j+1}(\varkappa R) J_{i+1}(\varkappa R) . \end{aligned} \tag{14}$$

Eqs. (13,14) give us a closed-form solution of the integral equation (5) for an arbitrary isotropic spectrum Φ_n of refractive-index fluctuations. So, we reduce the initial integral eq. (5) to the algebraic eigenvalue problem (13). Once the matrix $A_{j,i}^m$ is calculated, this problem can be solved making use of the well-known numerical methods (Press et al. 1988) that give us the needed coefficients $\beta_{j,n}^m$ and eigenvalues λ_m. In the next section we consider the solutions of the problem of interest for several models of Φ_n usually used in calculations.

3. KARHUNEN-LOEVE FUNCTIONS OF THE TURBULENCE-INDUCED PHASE DISTORTIONS

3.1. Kolmogorov Model

The Kolmogorov model is widely-used in calculations dealing with light propagation through the turbulent atmosphere. The Kolmogorov refractive-index spectrum Φ_n is given by

$$\Phi_n(\varkappa) = \varkappa^{-11/3}. \tag{15}$$

Substituting eq. (15) into eq. (14) and calculating the integral we have the following expression for the matrix $A_{j,i}^m$

$$\begin{aligned} A_{j,i}^m &= 0.49\pi \left(\frac{R}{2r_0}\right)^{5/3} (-1)^{(i+j-2m)/2} (1-\delta_{0i})(1-\delta_{0j})\sqrt{(i+1)(j+1)} \\ &\times \frac{\Gamma(14/3)\Gamma\left(\frac{j+i-5/3}{2}\right)}{\Gamma\left(\frac{j-i+17/3}{2}\right)\Gamma\left(\frac{i-j+17/3}{2}\right)\Gamma\left(\frac{j+i+23/3}{2}\right)} \quad , \end{aligned} \tag{16}$$

where Γ denotes the Gamma-function.

Eq. (16) allows calculation of the K-L functions for the case of Kolmogorov turbulence. However, despite of its extreme popularity, the Kolmogorov model does not work well enough when the effects of the outer scale of turbulence become pronounced (Voistekhovich 1995; Voistekhovich & Cuevas 1995). The last situation appears when the outer scale magnitude turns out to be comparable to or less than the size of the observation zone (in astronomical applications, such conditions are met in the case of large-aperture telescopes or long-based interferometry). For this reason, several outer-scale-dependent models have been suggested. All these models are, in fact, empirical generalizations of the Kolmogorov one. However, despite their empirical background, there exists many experimental evidences supporting the validity of these models (Bester et al. 1992; Dekens et al.1994; Buscher et al. 1995). In what follows, we consider two frequently-used outer scale models: the exponential model and the von Karman model.

3.2. Exponential Model

In the case of exponential model, the refractive-index spectrum is expressed as

$$\Phi_n(\varkappa) = \varkappa^{-11/3}\left[1 - \exp\left(-\varkappa^2/\varkappa_e^2\right)\right] , \tag{17}$$

where

$$\varkappa_e = 2\pi/L_0,$$

and L_0 denotes the outer scale of the turbulence.

The matrix $A^m_{j,i}$ occurring in eq. (14) is expressed as

$$A^m_{j,i} = 0.49\pi \left(\frac{R}{2r_0}\right)^{5/3} (-1)^{(i+j-2m)/2}(1-\delta_{0i})(1-\delta_{0j})\sqrt{(i+1)(j+1)}\times$$
$$\left[\frac{\Gamma(14/3)\,\Gamma\left(\frac{j+i-5/3}{2}\right)}{\Gamma\left(\frac{j-i+17/3}{2}\right)\Gamma\left(\frac{i-j+17/3}{2}\right)\Gamma\left(\frac{j+i+23/3}{2}\right)} - \left(\frac{\varkappa_e R}{2}\right)^{i+j-5/3} \frac{\Gamma\left(\frac{j+i-5/3}{2}\right)}{\Gamma(j+2)\Gamma(i+2)}\,{}_3F_3\right], \tag{18}$$

where ${}_3F_3$ is the generalized hypergeometric function(.....) given by

$${}_3F_3 \;=\; {}_3F_3\left(\frac{i+j+3}{2},\frac{i+j+4}{2},\frac{i+j-5/3}{2};i+2,j+2,i+j+3;-\varkappa_e^2R^2\right).$$

3.3. von Karman Model

The Von Karman spectrum is given by

$$\Phi_n(\varkappa) = \left(\varkappa^2+\varkappa_k^2\right)^{-11/6}. \tag{19}$$

We use the following relation suggested in Voitsekhovich (1995) between the parameters $\varkappa_k$ and $\varkappa_e$ of the von Karman and exponential models

$$\varkappa_k = 0.49\varkappa_e = 3.075/L_0. \tag{20}$$

Calculating the integral in eq. (15) with the spectrum (18) we get

$$A^m_{j,i} \;=\; 1.96\pi^{-2}\left(\frac{R}{r_0}\right)^{5/3}(-1)^{(i+j-2m)/2}(1-\delta_{0i})(1-\delta_{0j})\sqrt{(i+1)(j+1)}\;\times$$
$$\frac{2^{-11/3}\Gamma(14/3)\Gamma(\frac{j+i-5/3}{2})}{\Gamma(\frac{j-i+17/3}{2})\Gamma(\frac{i-j+17/3}{2})\Gamma(\frac{j+i+23/3}{2})}\times$$
$${}_3F_4\left(\frac{7}{3},\frac{17}{6},\frac{11}{6};\frac{11}{6}-\frac{i+j}{2},\frac{i-j}{2}+\frac{17}{6},\frac{j-i}{2}+\frac{17}{6},\frac{i+j}{2}+\frac{23}{6};\varkappa_k^2R^2\right)+ \tag{21}$$
$$(R\varkappa_k)^{-11/3}\left(\frac{\varkappa_k R}{2}\right)^{i+j+2}\frac{\Gamma\left(\frac{i+j+2}{2}\right)\Gamma\left(\frac{5/3-i-j}{2}\right)}{\Gamma(\frac{11}{6})\Gamma(i+2)\Gamma(j+2)}\times$$
$${}_3F_4\left(\frac{i+j+3}{2},\frac{i+j+4}{2},\frac{i+j+2}{2};\frac{i+j+1/3}{2},i+2,j+2,i+j+3;\varkappa_k^2R^2\right).$$

The von Karman model is more popular than the exponential one. As it has been shown (Voitsekhovich 1995), both models give very similar results in calculations (one will see in the next section that the same tendency appears also in our simulations). However, as can be seen by comparing eq. (21) to eq. (18), the results obtained with the von Karman model have a more complicated mathematical form that makes this model less convenient for applications.

4. SIMULATIONS: COMPARING THE THEORETICAL AND SIMULATED RESULTS

As it has been shown above (see eq. 4), the coefficients of the phase distortions expansion over the associated K-L functions are non-correlated. This property allows the simulation of the phase samples taking the superposition of K-L functions with random coefficients whose standard deviations are given by the corresponding eigenvalue $\lambda_{m,n}$. Mathematically, it means that the ensemble of phase distortion $S(\rho,\varphi)$ is given by

$$S(\rho,\varphi)=\sum_{n=1}^{N}\sum_{m=0}^{M}\lambda_{m,n}K_n^m(\rho)\left[\alpha_{m,n}\cos(m\varphi)+\beta_{m,n}\sin(m\varphi)\right] \quad , \tag{22}$$

where $\alpha_{m,n}, \beta_{m,n}$ are the normally distributed quantities with zero mean and unit variance.

The number of K-L functions needed for simulations depends on the type of the problem to be solved. This number can be estimated theoretically or from numerical experiments. Our numerical experiments based on the comparison of the theoretical structure functions to those ones obtained from simulations have shown that approximately 100 K-L functions ($N=10, M=10$) in the case of middle class telescopes (3.5-m) are needed; while this number has to be increased to 400 ($N=20, M=20$) for large telescopes. In what follows we refer to the simulated results as the experimental ones.

The validity of simulations has been verified by comparing the experimental structure functions to the theoretical ones. The following expressions for theoretical structure functions have been used (Voitsekhovich 1995). For the exponential model

$$Ds(\rho)=6.88\left(\frac{\rho}{r_0}\right)^{5/3}+20.56\,(\varkappa_e r_0)^{-5/3}\left[1-{}_1F_1\left(-\frac{5}{6};1;-\frac{\rho^2\varkappa_e^2}{4}\right)\right]; \tag{23}$$

and for the von Karman model

$$Ds(\rho)=6.88\left(\frac{\rho}{r_0}\right)^{5/3}{}_0F_1\left(;\frac{11}{6};-\frac{\rho^2\varkappa_k^2}{4}\right)+3.69\,(\varkappa_k r_0)^{-5/3}\left[1-{}_0F_1\left(;\frac{1}{6};-\frac{\rho^2\varkappa_k^2}{4}\right)\right]. \tag{24}$$

Experimental structure functions were calculated by averaging over 2000 simulated samples. The results of calculations are plotted in Figure 1. and Figure 2. The theoretical and experimental results can be seen to be in good agreement for a wide range of outer scale magnitudes. The effect of the outer scale is well pronounced, especially for small magnitudes of the outer scale, that can be seen comparing the Kolmogorov structure function to the outer-scale-dependent ones. The above results support the conclusion that the simulator developed is suitable for modelling atmospheric wavefront distortions for a wide range of ground-based telescope systems.

As an example we present some simulations for the 6.5-m telescope project that will be constructed in San Pedro Mártir (México). We have simulated the atmospherically induced phase distortions for visible, near infrared and infrared regions for different magnitudes of L_0. In these simulations we used only the Fried parameter, r_0, that depends on the wavelength in order to select different optical regions. A seeing of 0.7″ in the visible has been assumed. That corresponds to $r_0 = 0.15$ m in the visible region ($\lambda = 550$ nm), $r_0 = 0.25$ m in the I band ($\lambda = 850$ nm), and $r_0 = 0.5$ m in the near IR J band ($\lambda = 1500$ nm). The recent experimental

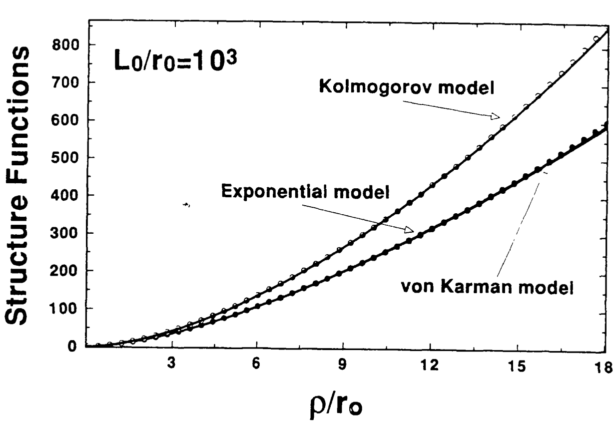

Fig. 1. Phase structure functions. Initial parts.

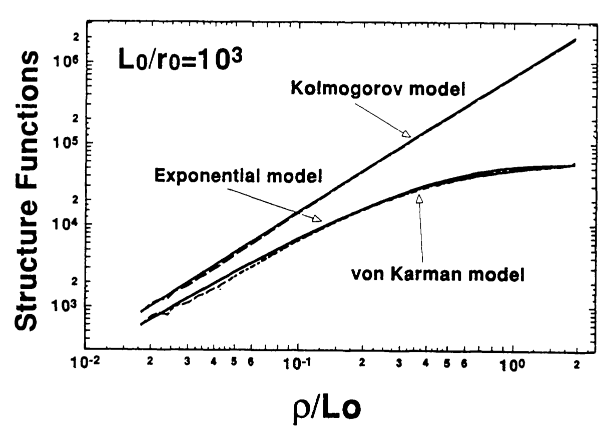

Fig. 2. Phase structure functions. Final parts.

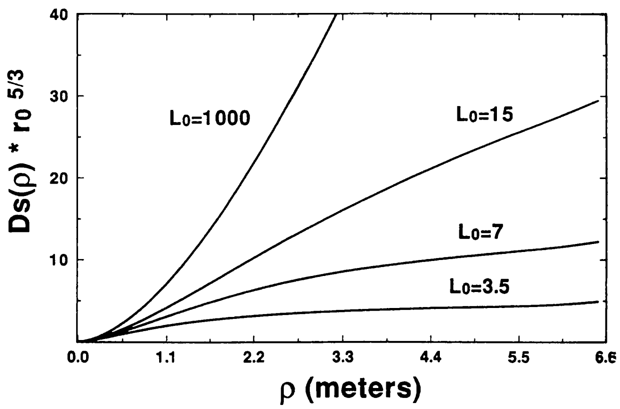

Fig. 3. Phase structure functions multiplied by $r_0^{5/3}$ for a 6.5-m telescope for different magnitudes of L_0.

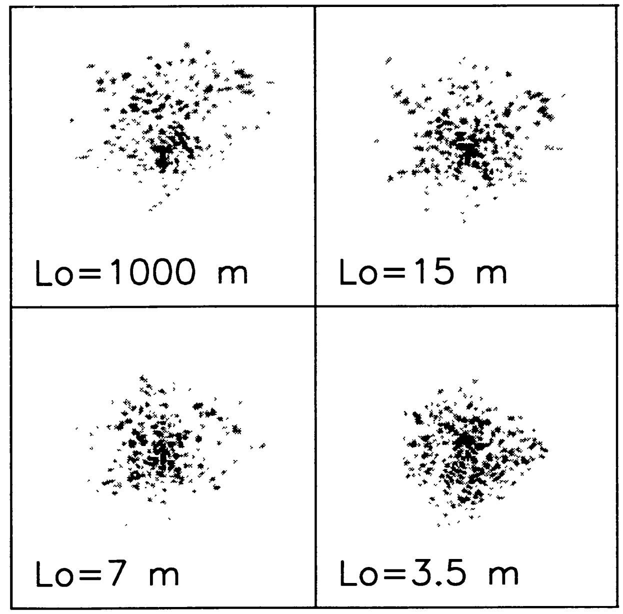

Fig. 4. Simulated speckle images for 6.5-m telescope in the visible region (λ = 550 nm) for different magnitudes of L_0 (r_0 = 0.15 m). Size of each image = 1.4 × 1.4 arcsec.

data show that L_0 has a finite size ranging from meters to tens of meters, so we have made simulations for $L_0 =$ 3.5, 7, 15 and 1000 m. The structure functions normalized by $r_0^{5/3}$ obtained from simulations are presented on Figure 3. As can be seen, the finite L_0 affects strongly the structure functions. It means that the finite L_0 must affect the point spread function and the images obtained by adaptive optic systems. The point spread function $PSF(\rightarrow x)$ can be calculated using the fast Fourier transform (FFT) of the telescope complex function P

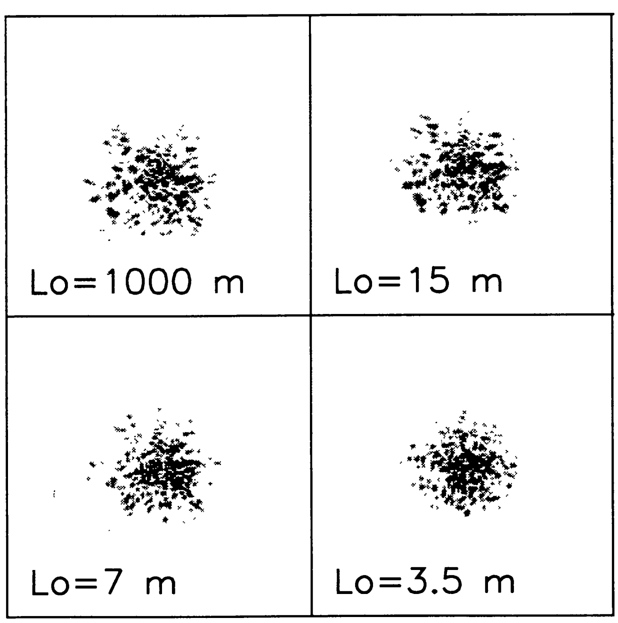

Fig. 5. Simulated speckle images for a 6.5-m telescope in the I band region (λ = 850 nm) for different magnitudes of L_0 (r_0 = 0.25 m). Size of each image = 2.1 × 2.1 arcsec.

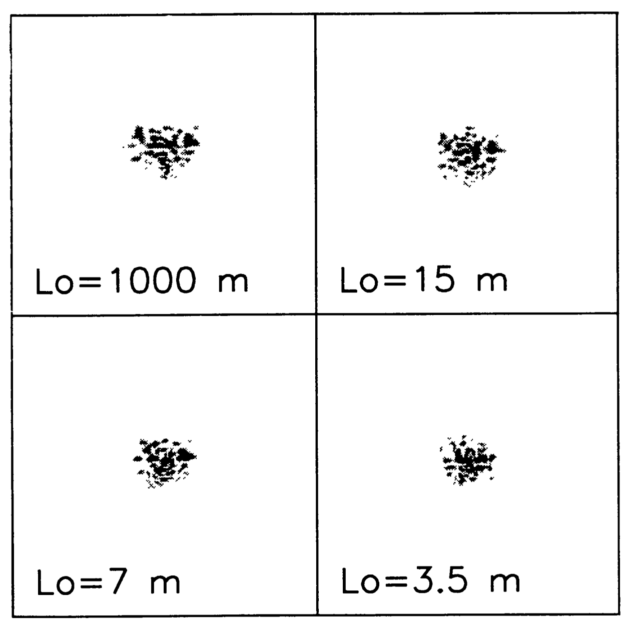

Fig. 6. Simulated speckle images for a 6.5-m telescope in the near J band region (λ = 1500 nm) for different magnitudes of L_0 (r_0 = 0.5 m).$Size of each image$ = 3.8× 3.8 arcsec.

$$P(\rho,\varphi)=\begin{cases}\exp\{\iota S(\rho,\varphi)\} & ,\text{if} \quad \rho\le R\\ 0 & ,\text{if} \quad \rho\ge R\end{cases}, \tag{25}$$

where $S(\rho,\varphi)$ is the simulated screen function.

In this form:

$$PSF\left(\overrightarrow{x}\right)=|F[\exp\{\iota S(\rho,\varphi)\}]|^2 \quad , \tag{26}$$

where F is the Fourier transform operator.

With only one phase screen representing one short exposure time it is possible to simulate speckle images. Typical speckle images obtained from simulations are presented in Figure 4, Figure 5, and Figure 6 for different atmospheric conditions. It can be shown that the bright speckles concentrate on the center of image when L_0 becomes comparable to the diameter of the telescope.

5. SUMMARY

The method suitable for deriving of the Karhunen-Loeve functions for any isotropic spectrum of the refractive-index fluctuations as a linear superposition of the Zernike polynomials has been presented. The approach developed allows a reduction of initial integral K-L equation to the homogeneous system of algebraic equations that gives the possibility to construct the K-L functions of interest with high accuracy. The analytical expressions needed for calculations of these functions have been presented for the cases of frequently-used turbulent models: the Kolmogorov model, the von Karman model and the exponential model. The obtained K-L functions have been used to develop the simulator that allows the modelling of the atmospherically induced phase distortions for a wide range of atmospheric conditions. Statistical characteristics of the simulated phase screens are in good agreement with theory. As an illustration, the results of modelling some properties of the 6.5-m telescope which is planned for construction on San Pedro Mártir have been presented.

REFERENCES

Afanasiyev, V. L., Balega, Y. Y., Orlov, V. G., & Vasyuk, V. A. 1991, A&A, 266, 15

Alloin, D., & Mariotti, J. M. 1993, in Proc. of the NATO ASI, Adaptive Optics for Astronomy, Carg'ese (Corsica) Series C: Vol. 423 (Dordrecht: Kluwer)

__________. 1988, in Proc. of the NATO ASI, Diffraction Limited Imaging with Very Large Telescopes, Carg'ese (Corsica) Series C: Vol. 274 (Dordrecht: Kluwer)

Babcock, H. W. 1953, PASP, 65, 229

Bester, M., Dnchi, W. C., Degiacomi, C. G., Greenhill, L. J., & Townes, C. H. 1992, OSA Technical Digest Series, 19, 48

Bouricius, G. M. B., & Clifford, S. F. 1970, J. Opt. Soc. Am., 60, 1484

Buscher, D. F., Armstrong, J. T., Hummel, C. A., Quirrenbach, A., Mozurkewich, D., Johnston, K. J., Denison, C. S., Colavita, M. M., & Shao, M. 1995, Appl. Opt., 34, 1081

Cannon, R. C. 1996, J. Opt. Soc. Am. A, 13, 862

Cliffod, S. F., Bouricius, G. M. B., Ochs, G. R., & Ackley, M. H. 1971, J. Opt. Soc. Am., 61, 1279

Close L., Roddier F., Northcott, M. J., Roddier C., & Graves J. E. 1997, AJ., 478, 766

Coulman, C. E., Vernin, J., Coqueugniot, Y., & Caccia, J. 1988, Appl. Opt., 27, 155

Dekens, F., Kirkman, D., Chanan, G., Mast, T., Nelson, J., Illingworth, G., & Wizinowich, P. 1994, Proc. SPIE 2201, ed. M. A. Ealey & F. Merkle (Billingham: SPIE), 303

Fried, D. L. 1966, J. Opt. Soc. Am., 56, 1372

Labeyrie, A. 1970, A& A, 6, 85

Loeve, M. 1955, Probability Theory (Princeton, NJ.: Van Nostrand)

McGlamery, B. L. 1976, Proc. SPIE, 74, 225

Nightingale, N. S., & Buscher, D. F. 1991, MNRAS, 251, 155

Noll, R. J. 1976, J. Opt. Soc. Am., 66, 207

Papoulis, A. 1984, Probability Random Variables and Stochastic Processes, International Student Edition

Pehlemann, E., Hofmann, K.-H., & Weigelt, G. 1992, A&A, 256, 701

Press, W. H., Flannery, B. P., Teukolsky, S. A., & Vetterling, W. T. 1988, Numerical Recipes in C (Cambridge: Cambridge U. Press)

Rigaut, F., & Gehring G. 1995, in The η Carinae Region: A Laboratory of Stellar Evolution, ed. V. Niemela, N. Morrell, & A. Feinstein, RevMexAASC, 2, 27

Roddier, N. 1990, Opt. Eng., 29, 1174

Roddier, F. 1981, The Effects of Atmospheric Turbulence in Optical Astronomy, Progress in Optics, XIX (North-Holland), 283

Roddier, C., Graves, J. E., Northcott, M. J., & Roddier, F. 1994, Proc. SPIE, 2199 (Billingham: SPIE), 1172

Roddier, C., Roddier, F., Northcott, M. J., Graves, J. E., & Kim, K. 1996, AJ., 463, 326

Takato, N., & Yamaguchi, I. 1995, J. Opt. Soc. Am., 12, 958

Tatarski, V. I. 1961, Wave Propagation in a Turbulent Medium (New York: McGraw-Hill)

Voitsekhovich, V. V. 1995, J. Opt. Soc. Am. A., 12, 1346

Voitsekhovich, V. V., & Cuevas, S. 1995, J. Opt. Soc. Am. A., 12, 2523
Wilson, R. N., Franza, F., & Noethe, L. 1987, J. of Modern Optics, 34, 485
Winker, D. M. 1991, J. Opt. Soc. Am. A., 8, 1568
Wang, J. Y., & Markey, J. K. 1978, J. Opt. Soc. Am., 68, 78

Salvador Cuevas, Valeri G. Orlov, and Valeri V. Voitsekhovich: Instituto de Astronomía, UNAM, Apartado Postal 70-264, 04510 México, D.F., México. (orlov@astroscu.unam.mx).